JOURNAL OF AGRICULTURAL AND FOOD CHEMISTRY

Crystallization Behavior and Texture of Trans-Containing and Trans-Free Palm Oil Based Confectionery Fats

VEERLE DE GRAEF,*,† IMOGEN FOUBERT,† KEVIN W. SMITH,‡ FRED W. CAIN,§ AND KOEN DEWETTINCK†

Ghent University, Faculty of Bioscience Engineering, Laboratory of Food Technology and Engineering, Coupure Links 653, B-9000 Gent, Belgium, Unilever Research Colworth, Sharnbrook, Bedfordshire, MK44 1LQ, U.K., and Loders Croklaan BV, Postbus 4, 1520AA Wormerveer, The Netherlands

The objective of this study was to gain insight into the role of trans fatty acids in determining the crystallization behavior and texture of palm-based confectionery fats. Therefore, the isothermal crystallization behavior of two series, each of three fats, one trans-containing and one trans-free, was examined by pNMR, DSC, and rheology. Furthermore, the hardness of these samples was examined at three different storage times at 10 °C. All of the trans free samples showed a two-step crystallization at 10 °C which is hypothesized to be an α-mediated β' crystallization for two of the samples and a fractionated crystallization in the β' polymorph for the third, while the trans-containing fats crystallized in a single step, probably a direct β' crystallization. The trans-containing fat series clearly crystallized faster than the trans-free fat series and also yielded higher hardness values at all storage times investigated. The presence of trans fatty acids seems to reduce the effect of compositional variations on the crystallization process. For the trans free fats, chemical composition was much more critical in determining the crystallization rate, the SFC, and the final hardness value.

KEYWORDS: Crystallization; rheology; microstructure; hardness; fat

INTRODUCTION

Recently, the pressure to ban trans fatty acids from food has dramatically increased because of their negative health implications. The major source of trans fatty acids is partially hydrogenated vegetable oils, which are frequently used in shortenings and confectionery products. To replace these partially hydrogenated fats, manufacturers have to turn to alternatives like palm oil and palm oil fractions. However, these alternatives should provide the same product functionality as the unwanted trans-containing fats.

The solid fat content (SFC) is a major factor determining the texture of fat, but the latter is also influenced by the polymorphism and the microstructure of the fat crystal network, which are in turn determined by the fat composition and crystallization conditions (*1*, *2*). Therefore, all these structure levels (primary crystallization, microstructural development, macroscopic properties) have to be studied to gain more insight in the effect of trans fatty acids on the final product texture. However, until now, few studies have addressed this issue in its full complexity. Foubert et al. (*3*) studied the relationship between crystallization, microstructure, and macroscopic properties in a trans-containing palm-based and trans-free lauric-based coating fat with DSC, microscopy and hardness measurements. Bell et al. (*4*) used a rheological approach to compare the crystallization of fats differing in composition (low trans and high trans) but with similar melting profiles.

The aim of this study was thus to gain more insight into the role of trans fatty acids on crystallization and texture of palm oil based confectionery fats. Therefore, a series of trans-containing and trans-free palm oil based confectionery fats were analyzed with several techniques to assess their crystallization behavior and texture at 10 °C. Differential scanning calorimetry (DSC) and pulsed nuclear magnetic resonance (pNMR) were applied to evaluate the primary crystallization, while oscillatory rheology provided information on primary crystallization, microstructural development, and macroscopic properties. Texture was evaluated in terms of hardness determined by penetrometry.

METHODS AND MATERIALS

Samples. Loders Croklaan (Wormerveer, The Netherlands) supplied two series of palm-based confectionery fats, one trans-containing (HTF: high trans fat) and one trans-free (NTF: no trans fat). Each fat series consists of three samples, each differing in chemical composition, thus

* Corresponding author. Tel: +32 9 264 61 98. Fax: +32 9 264 62 18. E-mail: veerle.degraef@ugent.be.
† Ghent University.
‡ Unilever Research Colworth.
§ Loders Croklaan BV.

10.1021/jf071967q CCC: $37.00
Published on Web 11/10/2007

Table 1. Fatty Acid Composition (wt %) of the High Trans Fat (HTF) and the No Trans Fat (NTF) Determined by Gas Chromatography

C12:0	C14:0	C16:0	C18:0	C18:1t	C18:1c	C18:2n-6	others	sat./unsat.	sat. +C18:1t/unsat.
HTF-1	0.31 ± 0.02	1.27 ± 0.04	39.98 ± 0.2	7.49 ± 0.05	31.44 ± 0.17	19.32 ± 0.10	0.19 ± 0.02	**0.97**	**4.17**
HTF-2	0.87 ± 0.02	1.47 ± 0.04	35.71 ± 0.09	7.53 ± 0.01	34.54 ± 0.23	19.58 ± 0.32	0.3 ± 0.03	**0.84**	**4.09**
HTF-3	0.28 ± 0.02	0.72 ± 0.01	23.86 ± 0.18	11.66 ± 0.01	41.71 ± 0.05	21.13 ± 0.13	0.64 ± 0.03	**0.58**	**3.70**
NTF-1	0.24 ± 0.01	1.26 ± 0.02	50.28 ± 0.07	5.04 ± 0.04	35.18 ± 0.06	7.67 ± 0.04	0.33 ± 0.01	**1.33**	**1.33**
NTF-2	0.16 ± 0.01	1.13 ± 0.03	54.06 ± 0.16	4.82 ± 0.02	33.36 ± 0.14	6.14 ± 0.02	0.33 ± 0.02	**1.52**	**1.52**
NTF-3	0.09 ± 0.01	0.94 ± 0.02	59.53 ± 0.16	6.04 ± 0.02	30.29 ± 0.15	2.77 ± 0.03	0.34 ± 0.01	**2.01**	**2.01**

leading to six different samples (HTF-1, HTF-2, HTF-3, NTF-1, NTF-2, and NTF-3). Samples were stored in the freezer.

Fatty Acid Composition. Fatty acid methyl esters (FAME) were produced according to the AOCS official method Ce 2-66 and subsequently analyzed on a Varian GC (Varian, Sint-Katelijne Waver, Belgium) with WCOT CP-sil88 column, split injector, and FID according to the AOCS official method Ce 1-62. Each analysis was executed in triplicate.

Triglyceride Composition. High-resolution separation for triglycerides was achieved using an Agilent 6890+ GC system fitted with an automated on column injection onto a Quadrex 15 m × 0.25 mm × 0.1 μm film 65% phenyl methyl silicone GC column. The samples were dissolved in isooctane at approximately 0.1 mg/mL. The injection volume was 0.1 μL. The helium carrier gas was set at a constant flow of 1 mL/minute. The oven program with injector in oven track mode was 80 °C for 0.5 min, ramping up to 330 at 50 °C/min, with triglyceride separation being achieved from 330 to 350 °C ramping at 1 °C/min. Detection was via FID.

The carbon number distribution was obtained using a Perkin-Elmer AUTOXL GC system fitted with a 10 m × 0.53 mm × 0.1 μL. Quadrex Scientific methyl–5% phenyl DB-5 capillary column. The samples were dissolved into isooctane at a concentration of approximately 2 mg/mL, and 0.5 μL was used as injection volume. The injector program was 70 °C for 0.1 min, ramping up to 350 at 200 °C/min and holding at 350 °C for 3 min The oven program was 200 °C at 0.0 min, ramping up to 325 at 10 °C/min, with triglyceride separation being achieved from 325 to 355 °C ramping at 5 °C/min. Helium was used as carrier gas and detection was via FID.

pNMR. pNMR experiments were performed with a Minispec pc 20 (Bruker, Karlsruhe, Germany). Liquefied fat was transferred into pNMR tubes and held at 65 °C for 30 min to eliminate any thermal history. Subsequently, the tubes were placed in a thermostatic water bath at 10 °C. Readings of the amount of solid fat were taken at appropriate time intervals, and a separate tube was used for each measurement. Each analysis was executed in triplicate.

Isothermal Crystallization via Stop-and-Return Technique (DSC). The isothermal crystallization curves were obtained with a TA Q1000 DSC (TA Instruments, New Castle, DE) with a refrigerated cooling system. The DSC was calibrated with indium (TA Instruments, New Castle, DE), azobenzene (Sigma-Aldrich, Bornem, Belgium), and undecane (Acros Organics, Geel, Belgium) before analyses. Nitrogen was used to purge the system. Fat (5–15 mg) was sealed in hermetic aluminum pans using sample preparation procedure B as described by Foubert et al. (*5*), and an empty pan was used as a reference. The applied time–temperature program for the isothermal crystallization curves was as follows: holding at 70 °C for 10 min to ensure a completely liquid state, cooling at 5 °C per min to the 10 °C (±0.05 °C), holding for the required crystallization time, and then heating at 20 °C per min to 70 °C. Thus, different crystallization times were allowed to occur before remelting. The area of the melting peak, which corresponds to the melting enthalpy, thus increased with increasing time at the 10 °C as the degree of previous crystallization increased. Hence, the degree of crystallization as a function of time at the crystallization temperature could be determined, despite the fact that some crystallization had occurred before the isothermal temperature was reached.

Microscopic Analyses. Microscopic analyses were conducted by the use of a Leitz Diaplan microscope (Leitz Diaplan, Leica, Germany) equipped with a Linkam PE94 temperature control system (Linkam, Surrey, U.K.). Samples were imaged with a Nikon Coolpix 4500 (Nikon, Melville, NY). To allow unhindered crystal growth, a cavity was formed on a glass slide by means of gluing some coverslips to the edges of the carrier glass. The molten sample was applied to this cavity and allowed to crystallize without a coverslip, thus allowing unhindered crystal growth in a three-dimensional space.

Oscillatory Rheology. Small deformation oscillatory experiments were performed on an AR2000 controlled stress rheometer (TA Instruments, Brussels, Belgium) using the starch pasting cell. Oscillation measurements were conducted at a constant frequency of 1 Hz and a strain of 4.500×10^{-3}. This very low strain was chosen to make sure that at every stage in the crystallization process measurements were performed within the linear viscoelastic region and to disturb the crystallization process as little as possible. The low frequency of 1 Hz was preferred in order to influence the crystallization as little as possible while maintaining enough data points (*6*). At the end each experiment an amplitude sweep was preformed on the crystallized sample to check whether the requirement of LVR was still fulfilled.

The melted sample was transferred into the cup and the following temperature profile was applied: keeping isothermally for 10 min at 70 °C to erase all crystal memory; cooling at 5 °C per min to 10 °C; oscillatory time sweep at 10 °C (isothermal period).

Rheograms were obtained by plotting the complex modulus (|G*|) and the phase angle (δ) of the crystallizing sample as a function of isothermal time at 10 °C. Each analysis was executed in triplicate.

Hardness (Penetration Test). Samples were cooled on a copper plate in which cooling water of 10 °C circulated and was placed inside a thermostatic cabinet at 10 °C to eliminate temperature fluctuations from the environment. Samples were crystallized at 10 °C for 30, 60, and 90 min after which the hardness was measured with a penetration test. This penetration test was performed on a Texture Analyzer TA 500 (Lloyd Instruments, Hampshire, U.K.) with a load cell of 500N and a cylindrical probe with a diameter of 4.51 mm (CNS Farnell, Hertfordshire, U.K.), penetrated the product at a constant speed of 10 mm per min to a distance of 10 mm. To ensure that measurement of the hardness at the specified temperature the texture analyzer was placed in a temperature-controlled cabinet at 10 °C (±0.5 °C) (Lovibond, Dortmund, Germany). Hardness was defined as the maximum penetration force (*N*), and each measurement was executed seven times.

RESULTS AND DISCUSSION

Characterization of the Samples: Fatty Acid Composition. **Table 1** presents the fatty acid composition of the trans-containing (HTF: high trans fat) and the trans-free (NTF: no trans fat) fat series. The HTF series contained 31−42% elaidic acid (C18:1trans), while for the NTF no trans fatty acid was detected. Both fat series were high in palmitic acid (C16:0) and oleic acid (C18:1c) due to their palm oil based nature. Within the HTF series, the fats differed mostly in C16:0 and C18:1t content and to a minor extent in amount of C18:0 and C18:1c. For the NTF series, the major differences occurred in C16:0 content and amount of unsaturated fatty acids. These compositional differences can also be represented by the ratio of saturated to unsaturated fatty acids. This ratio was the highest for NTF-3 and the lowest for HTF-3. If C18:1t is assumed to behave more like a saturated fatty acid than an unsaturated one; the ratio of saturated + C18:1t to unsaturated can also be calculated. This ratio yields the highest value for HTF-1 and the lowest for NTF-1.

Table 2. Carbon Number Distribution (wt %) of the High Trans Fat (HTF) and the No Trans Fat (NTF) Determined by Gas Chromatography[a]

	C42	C44	C46	C48	C50	C52	C54	C56	C58	C60
HTF-1	0.06	0.07	0.22	2.51	29.68	52.14	14.58	0.73	0.00	0.01
HTF-2	0.16	0.17	0.27	2.30	22.74	54.40	18.66	0.99	0.19	0.12
HTF-3	0.11	0.10	0.70	1.84	14.98	25.11	51.96	3.72	0.9	0.58
NTF-1	0.06	0.13	0.47	3.99	53.24	33.2	8.23	0.49	0.13	0.06
NTF-2	0.04	0.07	0.45	3.91	61.4	27.54	6.04	0.41	0.14	0.00
NTF-3	0.02	0.08	0.54	4.28	71.94	19.36	3.27	0.32	0.15	0.04

[a] Note that single measurements were made on each sample.

Table 3. Triglyceride composition (wt %) of No Trans Fat (NTF) Determined by High-Resolution Gas Chromatography[a]

		NTF-1	NTF-2	NTF-3
C46	MMP	0.33	0.38	0.47
	MOM	0.14	0.07	0.07
C48	PPP	1.41	1.63	2.48
	MOP	2.04	1.96	1.65
	MLP	0.54	0.33	0.15
C50	PPS	0.82	0.21	0.80
	POP	42.93	52.56	65.80
	PLP	9.30	8.38	5.18
	MLO	0.15	0.05	0.00
	MLL	0.24	0.31	0.35
C52	PSS	0.36	0.02	0.64
	POS	7.85	10.15	13.09
	POO	16.04	11.21	3.47
	PLS	1.79	1.28	0.95
	PLO	5.99	4.03	1.00
	PLL	1.23	0.86	0.20
C54	SSS	0.16	0.01	0.13
	SOS	1.10	1.43	2.04
	SOO + PLS	2.08	1.48	0.40
	OOO	2.66	1.92	0.33
	SLO	0.76	0.54	0.04
	OLO	1.27	0.62	0.13
	OLL	0.20	0.03	0.19
	others	0.61	0.56	0.44

[a] Note that positional isomers have not been separated and that single measurements were made on each sample.

The carbon number composition of the HTF and NTF series is displayed in **Table 2**. When comparing the two series, the HTF series proves to be higher in C52 and C54 compared to the NTF series but lower in C50. Within the HTF series, the amount of C48 and C50 decreased from HTF-1 to HTF-3, while C54 increased. The highest percentage of C54 was found in HTF-3. HTF-3 stood out from HTF-1 and HTF-2 as it was lower in C52 (25.11% compared to 52.14% and 54.40%, respectively) but high in C56 (3.72% compared to 0.73% and 0.99%, respectively). Within the NTF series, C52 and C54 decreased from NTF-1 to NTF-3, while C50 increased. NTF-3 also showed a slightly higher C48 compared to NTF-1 and NTF-2 (4.28% compared to 3.99% and 3.91%, respectively).

High-resolution GC analysis was unable to separate the wide range of cis–trans isomers present in the HTF samples, and therefore, only carbon number GC data can be reported for these samples. The triglyceride composition of the NTF-series, obtained with high resolution GC, is presented in **Table 3**. Within this series, the amount of PPP, POP, POS, and SOS increased from NTF-1 via NTF-2 to NTF-3, while the percentage of PLP, POO, PLO, SOO + PLS and OOO decreased.

Isothermal Primary Crystallization Behavior at 10 °C. The isothermal crystallization behavior at 10 °C of the two fat series was investigated with several techniques, namely DSC, pNMR, and oscillatory rheology.

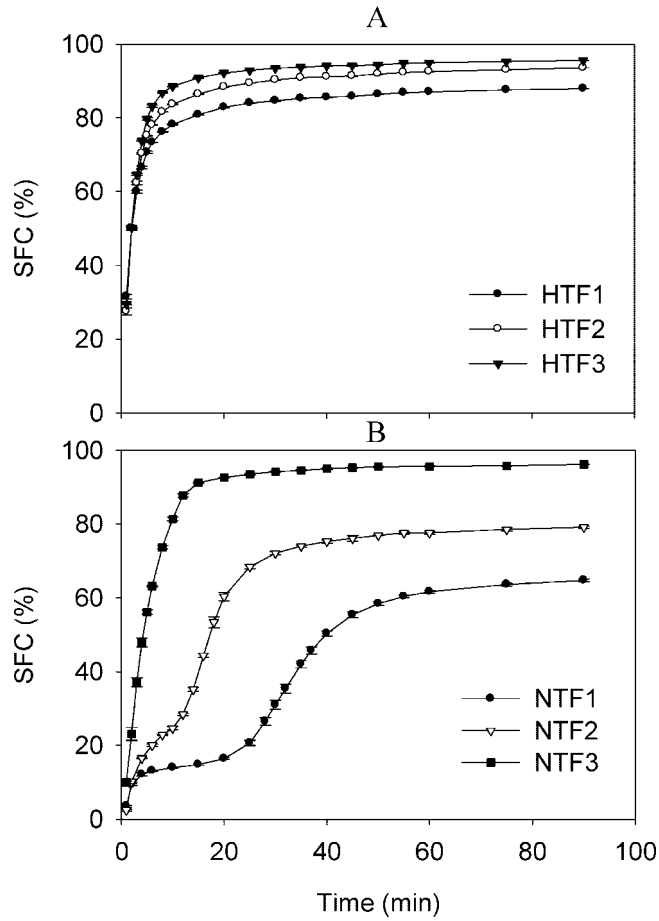

Figure 1. SFC of (**A**) HTF and (**B**) NTF as a function of time at 10 °C obtained with pNMR (NTF = no trans fat; HTF = high trans fat).

Figure 1 presents the SFC as a function of time at 10 °C for the HTF- (**Figure 1a**) and NTF series (**Figure 1b**). As can be seen in **Figure 1a**, the three HTF fats showed a very similar primary crystallization. They all started to crystallize very rapidly and quickly reached an equilibrium value which was quite high. This equilibrium value was significantly ($p = 0.05$) different within the HTF series: HTF-3 reached a slightly higher equilibrium value (95.50 ± 0.07%) compared to HTF-2 (93.51 ± 0.01%) and HTF-1 (87.89 ± 0.06%). These differences can be attributed to the different amount of trans fatty acid in the three HTF fats (**Table 1**), being lowest for HTF-1 and highest for HTF-3. Although HTF-3 had the lowest ratio of saturated fatty acids + C18:1t to unsaturated fatty acids, it reached the highest SFC equilibrium value, which is probably related to the higher amount of C18:1t as trans fatty acids tend to crystallize faster than their cis equivalents, as has been demonstrated in a recent study by Vereecken et al. (*7*).

However, with the ratio of saturated fatty acids + C18:1t to unsaturated fatty acids being rather similar for the three HTF fats, no major differences were expected, despite the differences in chemical composition. In carbon number composition (**Table 2**) the C54-content (higher melting) increases from HTF-1 to HTF-3, while the C48 and C50 content decreases. These compositional differences can be an explanation for the differences in primary crystallization.

The NTF series showed major differences in primary crystallization as is illustrated in **Figure 1b**. NTF-3 crystallized very rapidly and, like the HTF, quickly reached a high equilibrium value (96.14 ± 0.01%). NTF-2 and NTF-1 crystallized much slower, and their equilibrium value was significantly ($p = 0.05$)

lower, 79.14 ± 0.30% and 64.72 ± 0.46% respectively. Based in **Table 3**, it can be seen that NTF-3 is higher in PPP, POP, POS, and SOS compared to NTF-2 and NTF-1, respectively, which is in agreement with the order of crystallization.

Taking into account the ratio of saturated to unsaturated fatty acids (**Table 1**), NTF-3 is indeed expected to crystallize faster than NTF-2 and NTF-1. However, this ratio does not explain why the HTF-fats, having a lower ratio of saturated to unsaturated fatty acids, crystallized so much faster. A possible explanation lies in the presence of C18:1t in the HTF-series. Based on the structure of trans fatty acids, which is more similar to that of saturated fatty acids rather than to cis-unsaturated fatty acids, it might be assumed that they behave more as saturated fatty acids. The ratio of saturated fatty acids + C18:1t to unsaturated fatty acids (**Table 1**) is much higher for the HTF series compared to the NTF series, which is in agreement with the order of crystallization.

On the basis of **Figure 1**, it can also be assumed that the NTF and HTF series possess a different primary crystallization mechanism. In **Figure 1a**, the HTF-series display a single step primary crystallization, while in **Figure 1b**, NTF-1 and NTF-2 clearly exhibit a two-step primary crystallization. On the basis of **Figure 1b**, a single-step primary crystallization process could be assumed for NTF-3. In general, a two-step primary crystallization mechanism can be due to a polymorphic transformation, a fractionated crystallization, or a combination thereof.

The primary crystallization mechanism was further investigated with stop-and-return DSC experiments. The principle of the stop-and-return technique is to interrupt the primary isothermal crystallization at different moments in time and, subsequently, heat the sample to obtain the melting profile of the crystals formed during the immediately preceding isothermal period. Based on this melting profile, information on the primary crystallization process can be obtained.

Figure 2b represents the melting curves of NTF-3 at different isothermal times at 10 °C. Although **Figure 1b** did not reveal a two-step primary crystallization mechanism, **Figure 2b** proves otherwise. The melting endotherms clearly displays two minima (or negative peaks), one at 18 °C and one at 25 °C. The first peak was already present after 2 min of crystallization and gradually decreased at later times, with the second peak appearing as the first one decreased. Palm oil is known to exhibit a two-step crystallization below a certain cutoff temperature, which depends on composition. Below this cutoff temperature, palm oil is said to undergo an α mediated β' crystallization, while at higher temperatures β' crystals are directly formed from the melt (*8, 9*). The first peak in **Figure 2b** might thus be attributed to the α polymorph and the second peak to the β' polymorph, possibly with extra β' formation directly from the melt. **Figure 1b** already suggested a two-step primary crystallization for NTF-1 and NTF-2. Stop-and-return results confirmed that for NTF-3 this two-step primary crystallization was due to a polymorphic transition. For NTF-1 (**Figure 2c**), however, this two-step mechanism appeared to be caused by a fractionated crystallization into a high-melting and a low-melting fraction, possibly both directly in the β' polymorph. This is apparent since the high-melting peak appears first and grows a little before the low-melting peak appears and increases in size. This suggests a high-melting fraction begins to crystallize at the start, later joined by the lower-melting fraction. The difference in mechanism is most likely due to compositional differences as expressed in the carbon number profile (**Table 2**) and the triglyceride composition (**Table 3**). Compared to NTF-2 and NTF-3, NTF-1 has a lower percentage of PPP, POP, POS, and SOS, while being higher in PLP, POO, PLO, PLL, SOO + PLS, OOO, SLO, and OLO. It can thus be supposed that at 10 °C, NTF-2 and NTF-3 undergo an α mediated β' crystallization, while NTF-1 crystallizes directly in the β' polymorph, with the two-step character due to a lower melting and a high melting fraction.

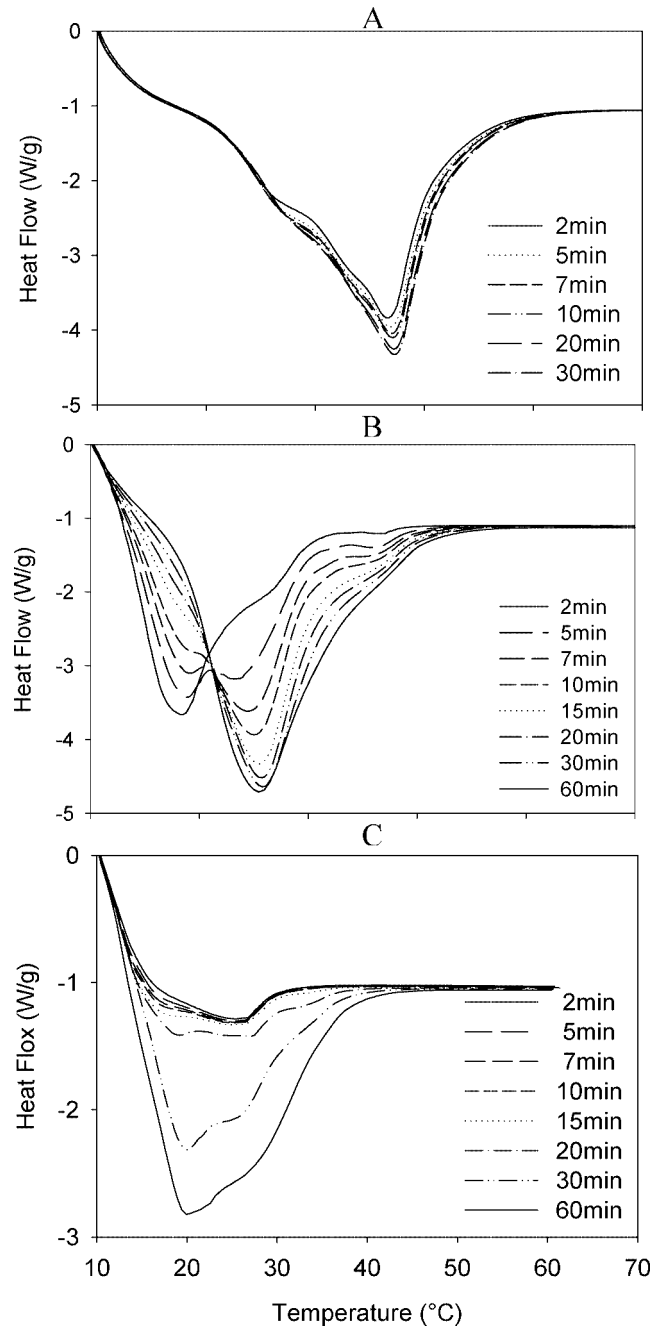

Figure 2. Melting curves of (**A**) HTF-2, (**B**) NTF-3, and (**C**) NTF-1 and at 10 °C obtained with DSC (NTF = no trans fat; HTF = high trans fat).

For the HTF-fats, a single-step primary crystallization process was hypothesized, which is illustrated in **Figure 2a**. **Figure 2a** shows the melting curves of HTF-2 at different isothermal times at 10 °C. In contrast to **Figure 2b**, only a single peak is present with a peak minimum at 37 °C, probably indicating a direct crystallization in a more stable polymorph. Based on these data, it cannot be concluded whether the HTF-fats crystallize in the β' or β polymorph. Taking into account that the HTF series is palm oil based, it is likely that the HTF samples crystallize directly in the β'-polymorph (*8, 10*).

The different primary crystallization mechanism of the NTF- and HTF-series could be explained by the difference in fatty acid composition. A higher ratio of saturated fatty acids + C18:1t to unsaturated fatty acids appeared to cause a direct crystallization in the β' polymorph.

Oscillatory Rheology at 10 °C. The isothermal crystallization at 10 °C was also investigated with oscillatory rheology. This technique allows recording all three steps of the crystallization process, namely primary crystallization, microstructural development of the fat crystal network, and macroscopic properties. The fat crystal network is formed by the aggregation of fat crystals through van der Waals attraction (*11, 12*). This aggregation process continues until a continuous three-dimensional network is formed. Fat crystals already start to aggregate at low volume fractions of crystallized fat, forming voluminous aggregates, while nucleation and crystal growth still go on (*12*). As a consequence of simultaneous crystallization and aggregation, a continuous network is already formed, while a substantial amount of fat still has to crystallize. This generally leads to sintering, i.e. the formation of solid bridges between aggregated crystals and aggregates (*11*). The number, size, and shape of the particles and large clusters will define the microstructure, which will in turn determine the macroscopic properties of the fat (*13*).

The complex modulus $|G^*|$, incorporating both the storage modulus G' and the loss modulus G'', can be used to evaluate the overall structure of the system. $|G^*|$ can be defined as the ratio of the shear stress to the applied deformation and consists of a real and an imaginary component, respectively, G' and G''. G' is denoted as the elastic, storage, or in-phase modulus and is a measurement for the solid nature of the sample. On the other hand, the viscous, loss or out-phase modulus G'' is an indication for the fluid character of the viscoelastic system. In a pure viscous system, such as a vegetable oil or completely melted palm oil, δ equals 90°. Once nucleation occurs and crystals start to grow, δ starts to decrease as the solid character of the crystallizing oil increases. This decrease can be quite drastically. At a δ above 45°, the sample displays a predominantly fluid character, while for values lower than 45°, the solid character prevails. Eventually, when the system becomes fully crystallized δ approaches zero (*6*).

Crystallization curves were obtained by plotting the complex modulus and the phase angle as a function of isothermal time at 10 °C, which is illustrated in **Figure 4**. As some of the samples began to crystallize during the cooling step, the cooling time is included as a negative isothermal time.

Figure 3a presents the phase angle and complex modulus of NTF-3. Although measurements are executed in triplicate, this graph represents a typical curve as there is very little variation among the repetitions.

The evolution of the phase angle in time can be divided in five different sections as indicated by the dotted lines. As shown by Toro-Vazquez et al. (*14, 15*) and De Graef et al. (*6*), these different sections can be attributed to crystallization into different polymorphic forms. The discussion of these sections is based on **Figure 3a** of NTF-3, but also applies to NTF-2.

Section 1: δ is close to 90°, indicating a fully melted sample.

Section 2: δ decreases sharply from 90° to 24°. This decrease can be attributed to crystallization in the α polymorph.

Section 3: δ remains more or less unchanged. The α crystals formed in section 1 are converted into β' crystals via a solid state transformation, as seen in the DSC results. The variation in phase angle during this step is probably caused by the crystallization heat released during section 1. This crystallization heat can induce a temperature rise, locally causing crystals to melt. This then leads to a loosening of the network structure and an increase in phase angle.

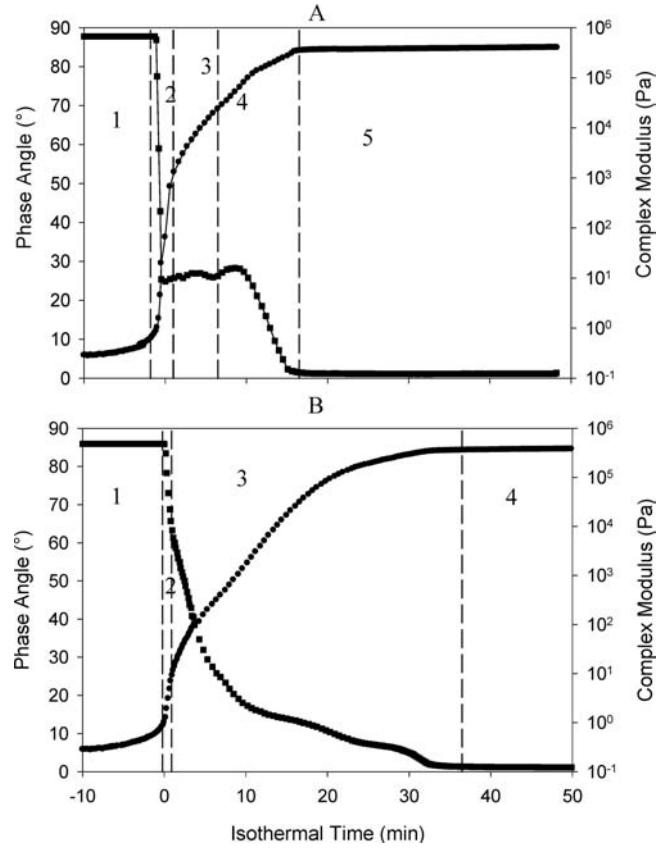

Figure 3. Phase angle (■) and complex modulus (●) of (**A**) NTF-3 and (**B**) NTF-1 as a function of isothermal time at 10 °C obtained with oscillatory rheology (NTF = no trans fat).

Section 4: δ decreases again to 1°. This decrease is caused by the formation of β' crystals directly from the melt, aggregation and network formation.

Section 5: δ remains at 1°, indicating a completely crystallized sample.

Also shown in **Figure 3a** is the complex modulus. The changes in complex modulus correspond with the time scale of events in the phase angle. In section 1, the low values illustrate the liquid state of the sample; in section 2, the fat gains structure as α crystals are formed; in sections 3 and 4, this increasing trend is maintained due to the polymorphic transition of α to β' crystals and the subsequent formation of β' crystals from the melt; and in section 5, the complex modulus reaches an equilibrium value which can be used to evaluate the macroscopic properties of the sample.

The increase in complex modulus and the decrease in phase angle are not only due to the primary crystallization but also to development of the microstructure by aggregation. These two processes cannot be completely separated. Walstra (*16*) already pointed out that ongoing crystallization and particularly recrystallization cause a growing together or sintering of the flocculated crystals, thereby greatly enhancing the strength of the bonds in the network, which can be seen as an increase in complex modulus. Sintering can already occur in a very early stage (*17*).

For NTF-1, phase angle and complex modulus behave quite differently, as presented in **Figure 3b**. As discussed earlier, NTF-1 has a different primary crystallization mechanism than NTF-2 and NTF-3: NTF-1 crystallizes into two fractions, both

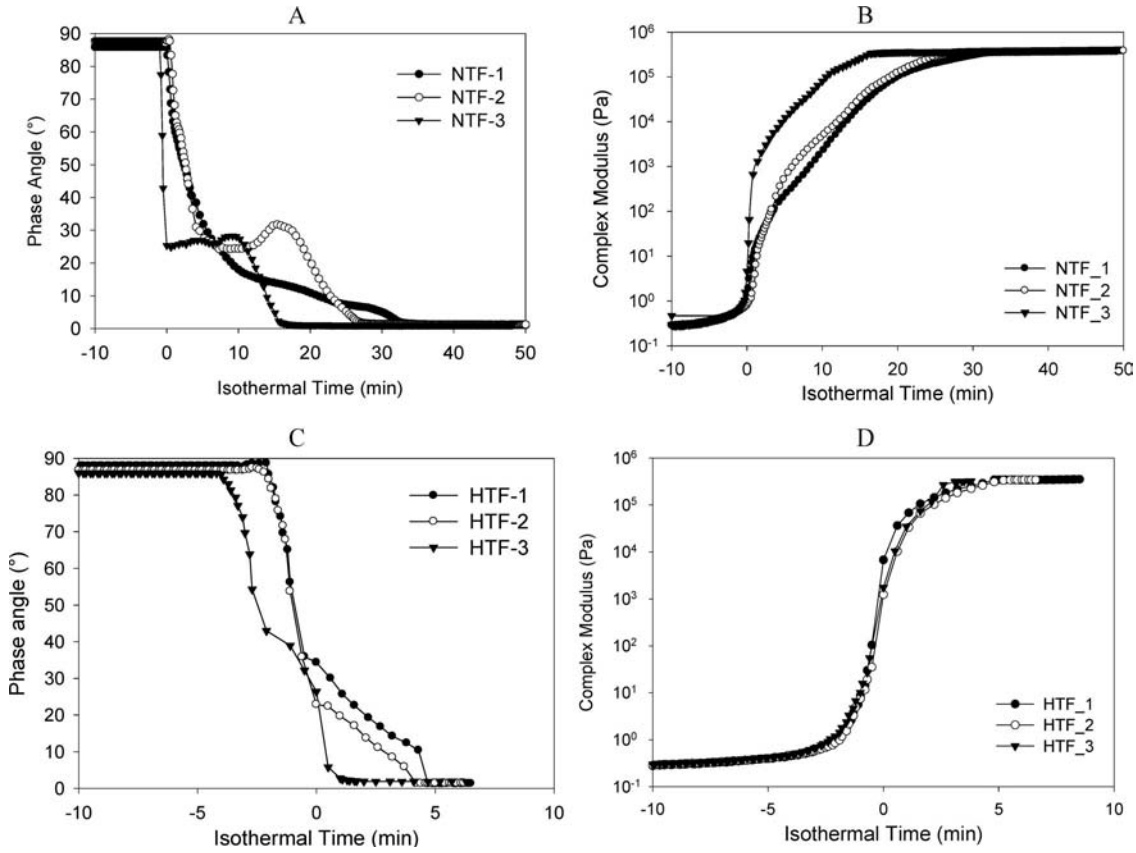

Figure 4. Phase angle (**A** and **C**) and complex modulus (**B** and **D**) of the NTF series and the HTF series, respectively, as a function of isothermal time at 10 °C obtained with oscillatory rheology (NTF = no trans fat; HTF = high trans fat).

assumed to be in the β' polymorph. This difference in primary crystallization mechanism can also be found in the rheological data:

Section 1: δ is close to 90° indicating a completely melted sample.

Section 2: δ decreases to about 65°, due to the crystallization of the higher melting fraction and aggregation of the crystals.

Section 3: δ further decreases to 1° due to crystallization of the lower melting triglycerides and network formation.

Section 4: δ is close to 0°, indicating a fully crystallized sample.

The complex modulus of NTF-1 is similar to that of NTF-3 as can be deduced from **Figure 4b**: thus, the difference in primary crystallization mechanism cannot be assessed on the basis of the complex modulus. When evaluating the complex moduli of the NTF series presented, it can be seen that the differences between these fats are mainly situated in the rate of increase of the complex modulus. In other words, the NTF fats develop a rather similar microstructure, but the time scale in which this happens differs. Polarized light microscopy (data not shown) revealed that aggregation was preceded by a period of nucleation and crystal growth (primary crystallization). The aggregates grew for some time before network formation occurred. For NTF-1, this network formation developed slowly, which agrees with the long and gradual decrease of the phase angle and increase in complex modulus. For NTF-2, network formation occurred slightly sooner, but the gradual increase in complex modulus is very similar to the one seen for NTF-1. On the other hand, network formation happened very quickly for NTF-3, which is in agreement with the rapid increase of the complex modulus in section 2 (**Figure 3a**).

For all of the NTF fats, the complex modulus reached an equilibrium value. NTF-3 attained an equilibrium value of $3.52 \times 10^5 \pm 2.64 \times 10^3$ Pa at 16 min isothermal time, while NTF-1 and NTF-2 reached their equilibrium values of $3.44 \times 10^5 \pm 5.03 \times 10^3$ Pa and $3.45 \times 10^5 \pm 1.73 \times 10^3$ Pa, respectively, at 34 and 28 min isothermal time. The equilibrium value of NTF-3 was significantly ($p = 0.05$) higher compared to NTF-1 and NTF-2, which did not significantly differ ($p = 0.05$).

For the HTF fats, the complex modulus increased rapidly as is illustrated in **Figure 4d**, indicating a rapid crystallization process. As has been discussed earlier, the HTF-fats showed a rapid single step primary crystallization. Based on the complex moduli, it can be assumed that the microstructural development is also very rapid and very similar for all HTF-fats. The phase angle (**Figure 4c**) shows an earlier onset of crystallization for HTF-3 and a rapid crystallization for all samples.

Polarized light microscopy (data not shown) revealed that during primary crystallization small crystals were formed which subsequently aggregated to a network structure. The strong increase in complex modulus coincided with this network formation. The similarity of the complex modulus indicates a similar microstructure for the HTF fats, based on which a similar hardness can be expected. As for the NTF fats, the complex modulus of the HTF fats attained an equilibrium value: $3.44 \times 10^5 \pm 4.58 \times 10^3$ Pa for HTF-1, $3.34 \times 10^5 \pm 8.08 \times 10^3$ Pa for HTF-2, and $3.20 \times 10^5 \pm 3.78 \times 10^3$ Pa. No significant ($p = 0.05$) differences in equilibrium value were found between HTF-1 and HTF-2, but the one of HTF-3 was significantly ($p = 0.05$) lower than those of HTF-1 and HTF-2, which agrees with the ratio of saturated fatty acids +C18:1t to unsaturated fatty acids for the HTF fats. This significant difference might be due to the fact that structure breakdown occurred when the equilibrium value was just reached. This structure breakdown would be due to the test conditions no longer being within the linear viscoelastic region after less than

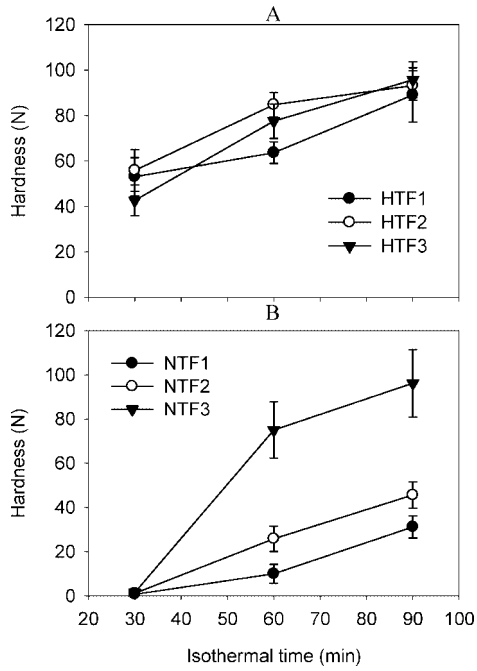

Figure 5. Hardness of (**A**) HTF and (**B**) NTF as a function of isothermal time at 10 °C obtained with penetrometry (NTF = no trans fat; HTF = high trans fat).

5 min isothermal time. For HTF-1 and HTF-2, this structural breakdown occurred some minutes later, which also indicated the similarity of the microstructure.

When comparing the rheological data of the HTF and NTF series, the main difference can be found in the time scale of events. Based on pNMR and DSC results, it was already clear that the HTF series crystallized much faster than the NTF series. This observation is confirmed by the rheological data. Comparing the end values of the complex modulus between the different fat series led to this result: HTF-3 < HTF-2=HTF-1=NTF-1=NTF-2 < NTF-3 ($p = 0.05$). This result might also be influenced by the fact that the HTF-sample could not be measured for the complete period due to structure breakdown.

Hardness as a Function of Time at 10 °C. Penetration tests were used to determine the hardness of the samples. The hardness of a fat is an important property that strongly influences the perceived texture of the fat containing food product (*18*).

Figure 5a shows the hardness of the HTF -series. At 30 and 90 min storage time, no significant ($p = 0.05$) differences were detected between the three HTF fats, while at 60 min the hardness of HTF-1 was significantly lower. It appears that differences in chemical composition were not translated into general differences in hardness. Based on the fatty acid profile (**Table 1**) an increasing hardness going from HTF-3 to HTF-1 could be expected as HTF-3 has the lowest ratio of saturated + C18:1t to unsaturated and HTF-1 the highest. Furthermore, HTF-3 reached the highest equilibrium SFC-value and HTF-1 the lowest.

Although the HTF reached their plateau SFC-value before 30 min isothermal time (**Figure 1a**), hardness continued to increase beyond this point, indicating SFC is not the sole factor to determine hardness (*19, 20*). However, it must be kept in mind that, when using different equipment to follow crystallization, comparison between results must be done with caution. Differences in sample weight or volume, equipment design and its impact on the thermodynamics of the system and, heat and mass transfer conditions existing in each measurement device, may affect the process to a different extent.

Other factors than SFC influencing mechanical properties of edible fats include the polymorphism of the solid state as well as the microstructure of the crystal network (*2, 21*). As the peak maximum in the melting profiles did not change as a function of time, polymorphism cannot be an explanation. A very plausible explanation for the change in hardness is sintering of the crystals. This leads to a further strengthening of the crystal network and, subsequently, an increase in hardness, without an increase in SFC (*12*).

The hardness of the NTF fats is presented in **Figure 5b**. At 60 and 90 min, the hardness of the NTF fats was significantly ($p = 0.05$) different, being at both storage times the highest for NTF-3 and the lowest for NTF-1. This agrees with the ratios saturated fatty acids + C18:1 to unsaturated fatty acids which increased form NTF-1 over NTF-2 to NTF-3. Thus, in the case of NTF fats, differences in composition were reflected by differences in hardness.

At 30 min isothermal time, all three NTF displayed very low hardness values. No significant differences were found, which is in contrast to the significant differences found in SFC. This observation indicates again that SFC is not the sole factor determining the hardness. Within the next 30 min, hardness increased significantly, especially for NTF-3. For NTF-1 and NTF-2, the increase was less pronounced. For NTF-2 and NTF-3, the increase in hardness between 30 and 60 min isothermal time cannot be explained by the SFC as an equilibrium value was reached before or around 30 min (**Figure 1b**). Because the peak maximum in the melting profiles did not shift, changes in polymorphism could not be the cause of this changing hardness. This change is likely to be due to phenomena like sintering (*12*). For NTF-1 on the other hand, the hardness increase between 30 and 60 min is linked with a significant increase in SFC, while this is not the case for the change in hardness from 60 to 90 min.

At 30 min storage time, the hardness of the NTF series was significantly ($p = 0.05$) lower than those of the HTF series, and HTF-3 was significantly ($p = 0.05$) lower than HTF-1 and HTF-2. At 60 min storage time this order has changed: NTF-1, NTF-2, and HTF-1 were significantly lower than HTF-3, which itself was significantly ($p = 0.05$) lower than NTF-3, HTF-1, and HTF-2. At 90 min storage time, NTF-3 was not significantly ($p = 0.05$) different from the HTF fats, which had a significantly ($p = 0.05$) higher hardness than NTF 1 and NTF-2. NTF-1 was significantly ($p = 0.05$) lower in hardness than NTF-2. So, from all the fats studied, the HTF series plus NTF-3 displayed the highest hardness after 90 min storage time, while the lowest values were found for NTF-1. The difference between the NTF fats can be explained on the basis of the chemical composition (**Table 2** and **Table 3**): NTF-3 has the highest percentages of PPP, POP, POS, and SOS, which are all rather high melting triglycerides, while these percentages are much lower in NTF-1. It appears that compositional differences in the HTF series do not cause major variations in hardness, while this is clearly the case for the NTF series. The presence of trans fat seems to flatten the compositional variations between the HTF series, possibly due to the presence of a greater number of triglycerides.

In summary, trans-containing palm oil based confectionery fats all crystallized much faster than their trans-free equivalents. Based on the stop-and-return DSC experiments, it could be concluded that the HTF series crystallized directly into a more stable polymorph, most likely β'. Although the HTF series differed in chemical composition, this difference was not

reflected in major variations in SFC, or in network formation, as expressed by the complex modulus, or in hardness. The presence of trans fat seems to reduce the influence of compositional variations to some degree.

The trans free palm oil based confectionery fats showed more differences. The stop-and-return experiments revealed different mechanisms of primary crystallization: NTF-2 and NTF-3 showed a two-step primary crystallization of polymorphic nature, while for NTF-1 the two-step process was due to crystallization in a high-melting and a low-melting fraction. For the NTF series, differences in chemical composition led to differences in SFC, network formation, and hardness. NTF-3, which has the highest ratio saturated to unsaturated fatty acid, showed the highest SFC value, the fastest network formation (increase in complex modulus) and the highest hardness values. On the basis of these results, NTF-3 behaved similar to the HTF fats. For the NTF series, differences in chemical composition had a major influence on the crystallization process.

Manufacturers have to be aware that, when replacing trans-containing fats with their trans-free alternatives, differences in chemical composition between these alternatives can have a tremendous effect on the final product quality. The formulation of a suitable alternative is, therefore, not straightforward. In addition, some modification of processing conditions might be anticipated.

ABBREVIATIONS USED

NTF, no trans fat; HTF, high trans fat; FAME, fatty methyl esters.

ACKNOWLEDGMENT

Lien Balduyck is acknowledged for performing many of the analyses.

LITERATURE CITED

(1) Marangoni, A. G.; Hartel, R. W. Visualization and structural analysis of fat crystal networks. *Food Technol.* **1998**, *52*, 46–51.

(2) Marangoni, A. G.; Narine, S. S. Identifying key structural indicators of mechanical strength in networks of fat crystals. *Food Res. Int.* **2002**, *35*, 957–969.

(3) Foubert, I.; Vereecken, J.; Smith, K. W.; Dewettinck, K. Relationship between crystallization behavior, microstructure, and macroscopic properties in trans containing and trans free coating fats and coating. *J. Agric. Food Chem.* **2006**, *54*, 7256–7262.

(4) Bell, A.; Gordon, M. H.; Jirasubkunakorn, W.; Smith, K. W. Effects of composition on fat rheology and crystallisation. *Food Chem.* **2007**, *101*, 799–805.

(5) Foubert, I.; Vanrolleghem, P. A.; Dewettinck, K. A differential scanning calorimetry method to determine the isothermal crystallization kinetics of cocoa butter. *Thermochim. Acta* **2003**, *400*, 131–142.

(6) De Graef, V.; Dewettinck, K.; Verbeken, D.; Foubert, I. Rheological behaviour of crystallizing palm oil. *Eur. J. Lipid Sci. Techn.* **2006**, *108*, 864–870.

(7) Vereecken, J.; Foubert, I.; Smith, K. W.; Dewettinck, K. Relationship between crystallization behavior, microstructure, and macroscopic properties in trans-containing and trans-free filling fats and fillings. *J. Agric. Food Chem.* **2007**, *55*, 7793–7801.

(8) Chen, C. W.; Lai, O. M.; Ghazali, H. M.; Chong, C. L. Isothermal crystallization kinetics of refined palm oil. *J. Am. Oil Chem. Soc.* **2002**, *79*, 403–410.

(9) Mazzanti, G.; Marangoni, A. G.; Idziak, S. H. J., Modeling phase transitions during the crystallization of a multicomponent fat under shear. *Phys. Rev. E* **2005**, 71, -.

(10) Yap, P. H.; Deman, J. M.; Deman, L. Polymorphism of Palm Oil and Palm Oil Products. *J. Am. Oil Chem. Soc.* **1989**, *66*, 693–697.

(11) Kloek, W. Properties of fats in relation to their crystallization. Ph.D. Thesis. Wageningen, The Netherlands, 1998.

(12) Walstra, P.; Kloek, W.; van Vliet, T. Fat crystal networks. In *Crystallization processes in fats and lipid systems*; Garti, N. S. K., Ed.; Marcel Dekker, Inc.: New York, 2001; pp 289–321.

(13) Marangoni, A. Special issue of FRI-crystallization, structure and functionality of fats. *Food Res. Int.* **2002**, *35*, 907–908.

(14) Toro-Vazquez, J.; Herrera-Coronado, V.; Dibildox-Alvarado, E.; Charo-Alonso, M.; Gomez-Aldapa, C. Induction time of crystallization in vegetable oils, comparative measurements by differential scanning calorimetry and diffusive light scattering. *J. Food Sci.* **2002**, *67*, 1057–1065.

(15) Toro-Vazquez, J. F.; Perez-Martinez, D.; Dibildox-Alvarado, E.; Charo-Alonso, M.; Reyes-Hernandez, J. Rheometry and polymorphism of cocoa butter during crystallization under static and stirring conditions. *J. Am. Oil Chem. Soc.* **2004**, *81*, 195–202.

(16) Walstra, P. Fat crystallization. In *Food Structure and Behaviour*; Blanshard, J. M. V., Lillford, P. L., Eds.; Academic Press: London, 1987; pp 67–85.

(17) Johansson, D.; Bergenstahl, B. Sintering of Fat Crystal Networks in Oil during Post-Crystallization Processes. *J. Am. Oil Chem. Soc.* **1995**, *72*, 911–920.

(18) Brunello, N.; McGauley, S. E.; Marangoni, A. Mechanical properties of cocoa butter in relation to its crystallization behavior and microstructure. *Food Sci. Technol.* **2003**, *36*, 525–532.

(19) Narine, S. S.; Marangoni, A. G. Mechanical and structural model of fractal networks of fat crystals at low deformations. *Phys. Rev. E* **1999**, *60*, 6991–7000.

(20) Narine, S. S.; Marangoni, A. G. Relating structure of fat crystal networks to mechanical properties: a review. *Food Res. Int.* **1999**, *32*, 227–248.

(21) Braipson-Danthine, S.; Deroanne, C. Influence of SFC, microstructure and polymorphism on texture (hardness) of binary blends of fats involved in the preparation of industrial shortenings. *Food Res. Int.* **2004**, *37*, 941–948.

Received for review July 2, 2007. Revised manuscript received October 8, 2007. Accepted October 8, 2007. This research was supported by a Ph.D. grant for V.D.G. from the Institute for the Promotion of Innovation by Science and Technology in Flanders (IWT). I.F. is a Postdoctoral Fellow of the Fund for Scientific Research-Flanders (F.W.O.-Vlaanderen).

JF071967Q